# Supplemental Material

## Acute TNF-induced repression of cell identity genes is mediated by NFκB-directed redistribution of cofactors from super-enhancers

Søren Fisker Schmidt,[1,3] Bjørk Ditlev Larsen,[1,3] Anne Loft,[1] Ronni Nielsen,[1] Jesper Grud Skat Madsen,[1,2] and Susanne Mandrup[1]

[1] University of Southern Denmark, Department of Biochemistry and Molecular Biology, Campusvej 55, 5230 Odense M, Denmark; [2] The Novo Nordisk Foundation Center for Basic Metabolic Research, University of Copenhagen, DK-2200 Copenhagen, Denmark.

[3] Equal contribution

Corresponding author:
Susanne Mandrup (s.mandrup@bmb.sdu.dk)

# Content of Supplemental Material

## Supplemental Figures and Tables

| **Figures** | **Related to** |
|---|---|
| Figure S1 | Figure 1 |
| Figure S2 | Figure 2 |
| Figure S3 | Figure 3 |
| Figure S4 | Figure 4 |
| Figure S5 | Figure 5 |
| Figure S6 | Figure 6 |
| | |
| **Tables** | **Related to** |
| Table S1 | Figure 1 |
| Table S2 | Figure S1, Figure 2, and Figure S2 |
| Table S3 | Figure S4 and Figure 6 |

## Supplemental Methods

## Supplemental References

# Fig. S1

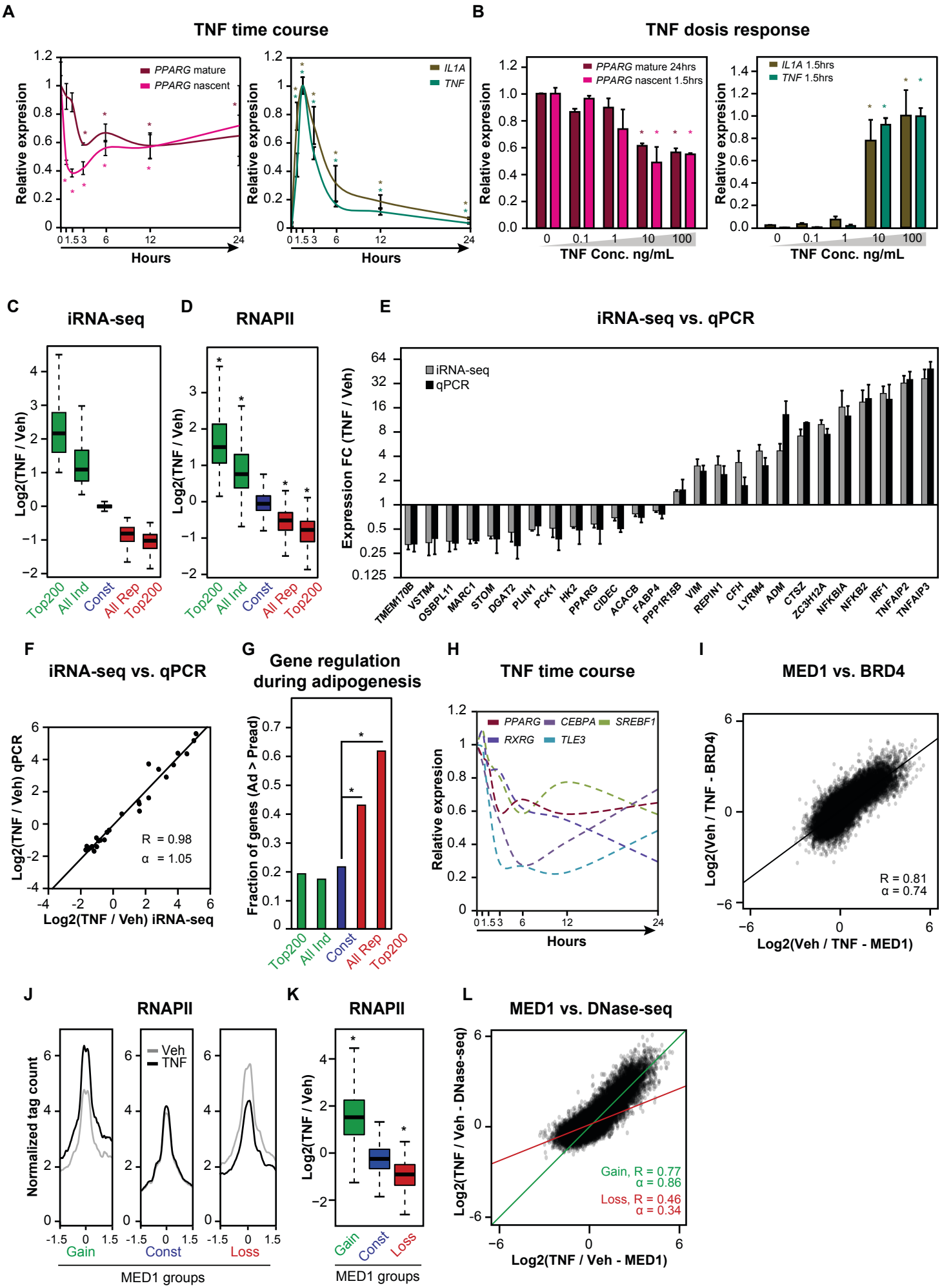
A
TNF time course
PPARG mature
PPARG nascent
IL1A
TNF
Relative expression
Hours
B
TNF dosis response
PPARG mature 24hrs
PPARG nascent 1.5hrs
IL1A 1.5hrs
TNF 1.5hrs
TNF Conc. ng/mL
C
iRNA-seq
Log2(TNF / Veh)
Top200
All Ind
Const
All Rep
Top200
D
RNAPII
E
iRNA-seq vs. qPCR
iRNA-seq
qPCR
Expression FC (TNF / Veh)
TMEM170B
VSTM4
OSBPL11
MARC1
STOM
DGAT2
PLIN1
PCK1
HK2
PPARG
CIDEC
ACACB
FABP4
PPP1R15B
VIM
REPIN1
CFH
LYRM4
ADM
CTSZ
ZC3H12A
NFKBIA
NFKB2
IRF1
TNFAIP2
TNFAIP3
F
iRNA-seq vs. qPCR
Log2(TNF / Veh) qPCR
Log2(TNF / Veh) iRNA-seq
R = 0.98
α = 1.05
G
Gene regulation during adipogenesis
Fraction of genes (Ad > Pread)
H
TNF time course
PPARG
CEBPA
SREBF1
RXRG
TLE3
Relative expression
Hours
I
MED1 vs. BRD4
Log2(Veh / TNF - BRD4)
Log2(Veh / TNF - MED1)
R = 0.81
α = 0.74
J
RNAPII
Normalized tag count
Veh
TNF
Gain
Const
Loss
MED1 groups
K
RNAPII
Log2(TNF / Veh)
Gain
Const
Loss
MED1 groups
L
MED1 vs. DNase-seq
Log2(TNF / Veh - DNase-seq)
Log2(TNF / Veh - MED1)
Gain, R = 0.77
α = 0.86
Loss, R = 0.46
α = 0.34

**Figure S1: Related to Figure 1**

**A:** Time course investigation of the effect of TNF on RNA expression of *PPARG* and inflammatory genes in SGBS adipocytes after 0, 0.75, 1.5, 3, 6, 12 and 24 hours treatment with TNF. RNA was extracted and quantified by qPCR. Lines represent TBP-normalized levels of *PPARG* mRNA and pre-mRNA (left) and *IL1A* and *TNF* mRNA (right) for all time points relative to the 0 hour and 1.5 hour time point, respectively. Data are represented as mean ± standard deviation, n=3. p-value relative to 0 hour:* < 0.05, Students t-test.

**B:** Dose-response investigation of the effect of TNF on RNA expression of *PPARG* and inflammatory genes in SGBS adipocytes after 0, 0.1, 1, 10, 100 ng/mL TNF for 1.5 or 24 hours. Bars represent TBP-normalized levels of *PPARG* mRNA and pre-mRNA levels after 24 and 1.5 hours, respectively (left) and *IL1A* and *TNF* mRNA levels after 1.5 hours (right) as determined by qPCR. Expression levels are relative to 0 (for *PPARG*) and 10 ng/mL TNF (IL1A and TNF), respectively. Data are represented as mean ± range, n=2. p-value relative to 0 ng/ml :* < 0.05, Students t-test.

**C:** Boxplot showing log2 fold change (TNF/Veh) in intron tag counts for TNF-induced (Ind), TNF-repressed (Rep) and constitutive (Const) gene groups defined in Fig. 1A. Top 200 regulated genes were defined as those with the smallest FDR.

**D:** Boxplot showing log2 fold change in RNAPII occupancy for TNF-regulated and constitutive genes defined in Fig. 1A. p-value compared to constitutive: *<2.2E-16, Wilcoxon rank sum test

**E+F**: Barplot (E) and scatterplot (F) illustrating correlation between TNF-induced changes in transcription assessed by iRNA-seq vs. qPCR with intron-targeting primers. A subset of 26 genes was selected based on their iRNA-seq-estimated fold changes to achieve coverage across the dynamic range of the TNF response. Data are represented as mean ± standard deviation of several biological replicates, iRNA-seq: n=3, qPCR: n=3-7.

**F**: Bar diagram representing the fraction of TNF-regulated and constitutive gene groups defined in Fig. 1A that are significantly upregulated during adipogenesis (FDR<0.01). p-value: *<2.2E-16, Pearson's Chi-squared test.

**G:** Time course investigation of the effect of TNF on expression of transcription factors expressed in SGBS adipocytes after 0, 0.75, 1.5, 3, 6, 12 and 24 hours treatment with TNF. Lines represent TBP-normalized levels of *PPARG, CEBPA, SREBF1, RXRG,* and *TLE3* mRNA as determined by qPCR for all time points relative to the 0 hour time point.

**H:** Scatterplot illustrating correlation between TNF-induced changes in MED1 occupancy and BRD4 occupancy. Black line represents the Pearson best fit line for correlation between BRD4 and MED1 signal (R=0.81, α=0.74 P<2.2E-16).

**I:** Aggregate plots showing RNAPII occupancy in a 3kb window around the center of intergenic TNF-regulated and constant MED1 sites defined in Fig. 1D.

**J:** Boxplot representing log2 fold change in RNAPII occupancy at intergenic TNF-regulated and constant MED1 sites defined in Fig. 1D. Tags were counted in a region of 1kb around the MED1 peak center and only sites with >8 RNAPII tags pr. 10 million tags in at least one condition were analyzed. p-value: *<2.2E-16, Wilcoxon rank sum test.

**K:** Scatterplot illustrating correlation between TNF-induced changes in MED1 occupancy and chromatin accessibility (DNase-seq). Green and red lines represent the Pearson best fit line for MED1 sites with gain (R=0.78, α=0.86, P<2.2E-16) and loss (R=0.46, α=0.34, P<2.2E-16) of MED1, respectively.

# Fig. S2

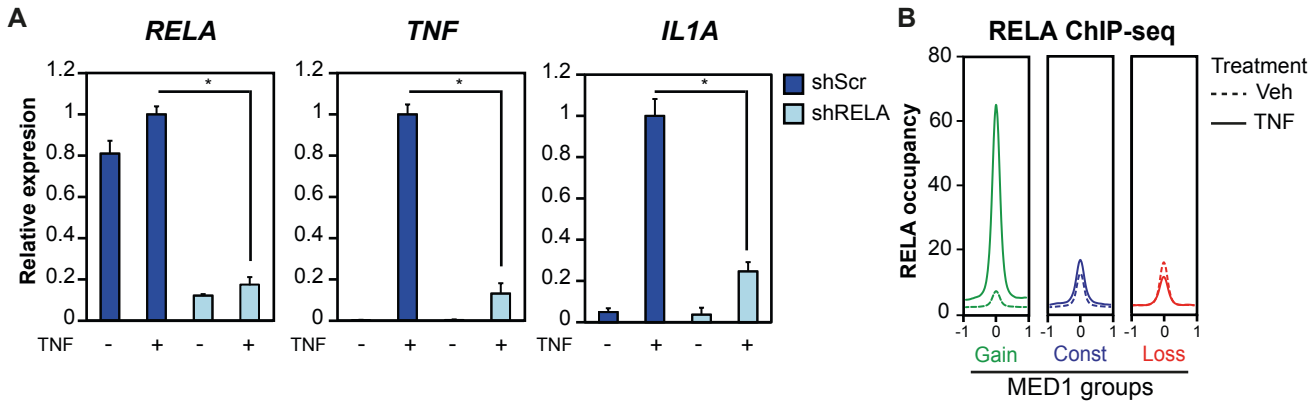


**Figure S2: Related to Figure 2**

Investigation of the role of NFκB in mediating the effects of TNF in SGBS adipocytes.

**A:** Bar diagrams representing TBP-normalized mRNA levels of *RELA*, *TNF*, and *IL1A* in SGBS cells transduced with lentivira expressing shRNA targeting *RELA* (shRELA, light blue) or scramble shRNA (shScr, dark blue) at day 6 and treated with vehicle or TNF for 90 min at day 10 of differentiation. Expression is normalized to mRNA levels in TNF-treated cells expressing scramble shRNA. Data are represented as mean±SD. n=3. *<0.05, student's t-test.

**B:** Aggregate plots showing RELA occupancy at enhancers in SGBS adipocytes treated with TNF or vehicle (Veh) for 60 min at day 10 of differentiation. Enhancers are grouped according to whether they gain (green), lose (red) or have constant (blue) MED1 binding following TNF exposure (defined in Fig. 1D).

# Fig. S3

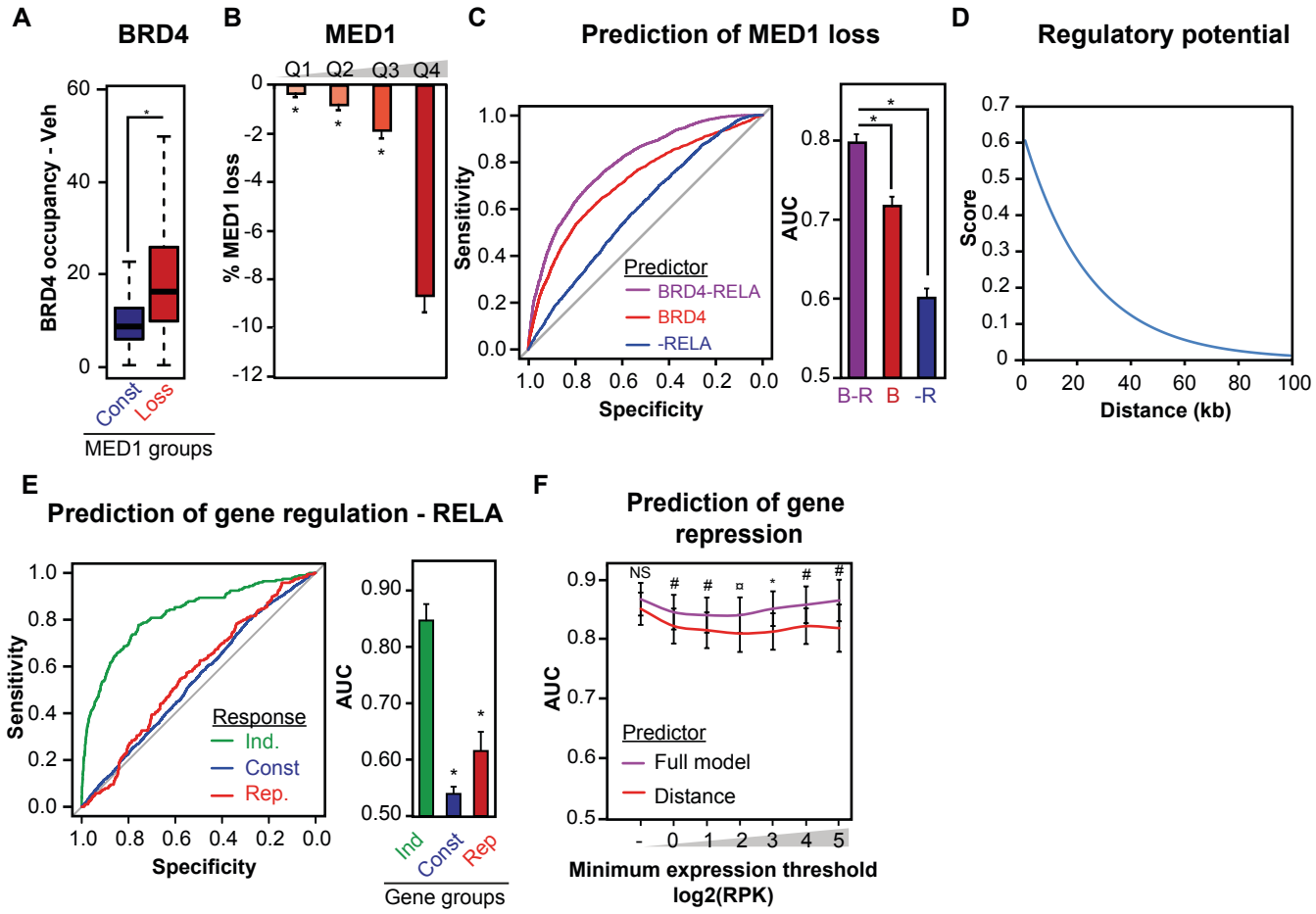


**Figure S3: Related to Figure 3**

Development of models for prediction of gene regulation in SGBS adipocytes based on MED1 and RELA occupancy and distance to TSS.

**A:** Boxplot showing BRD4 occupancy in vehicle-treated cells at sites that display constant occupancy or loss of MED1 upon TNF exposure. p-value:*<2.2E-16, Wilcoxon rank sum test.

**B:** Bar diagrams representing mean absolute loss of MED1 following TNF exposure for MED1 sites divided into quartiles based on MED1 occupancies in vehicle-treated SGBS adipocytes. Error bars represent 95% confidence interval around the mean. p-value compared to Q4:*<2.2E-16, Welch's t-test.

**C:** ROC-curves and bar diagrams representing prediction of MED1 loss as defined in Fig. 1D based on RELA occupancy in TNF-treated cells (blue), BRD4 occupancy in vehicle-treated cells (red), or subtracted occupancies (purple). Bar diagrams represent the AUC for each ROC-curve with error bars representing the 95% confidence interval of the AUC determined by DeLongs test. p-value:*<2.2E-16, DeLongs test.

**D:** Distance scores for each promoter-enhancer pair were calculated using the formula: Score = exp(-0.5+4*d/100000), where d is the distance in bp from promoter to enhancer.

**E:** ROC-curves for RELA occupancy-based prediction of the top 200 genes induced (green) and repressed (red) by TNF (defined in Supplemental Fig. S1C). As a control, constitutive genes (blue) were also predicted. Bar diagrams show the AUC for each ROC-curve with error bars representing the 95% confidence interval of the AUC determined by DeLongs test. p-value compared to induced:*<2.2E-16, determined by bootstrapping.

**F:** Line plots representing the dependency between minimum transcription thresholds and ROC AUCs for the prediction of top 200 repressed genes by TNF with the 'full model' (purple) (defined in Fig. 4G) and a 'distance model' (red) based solely on summarized distance scores for each gene (defined in Fig. 4I). Error bars represent the 95% confidence interval of the AUC determined by DeLongs test. p-value: #=p<5E-2, ¤=<5E-3, *=p<5E-4, DeLongs test.

# Fig. S4

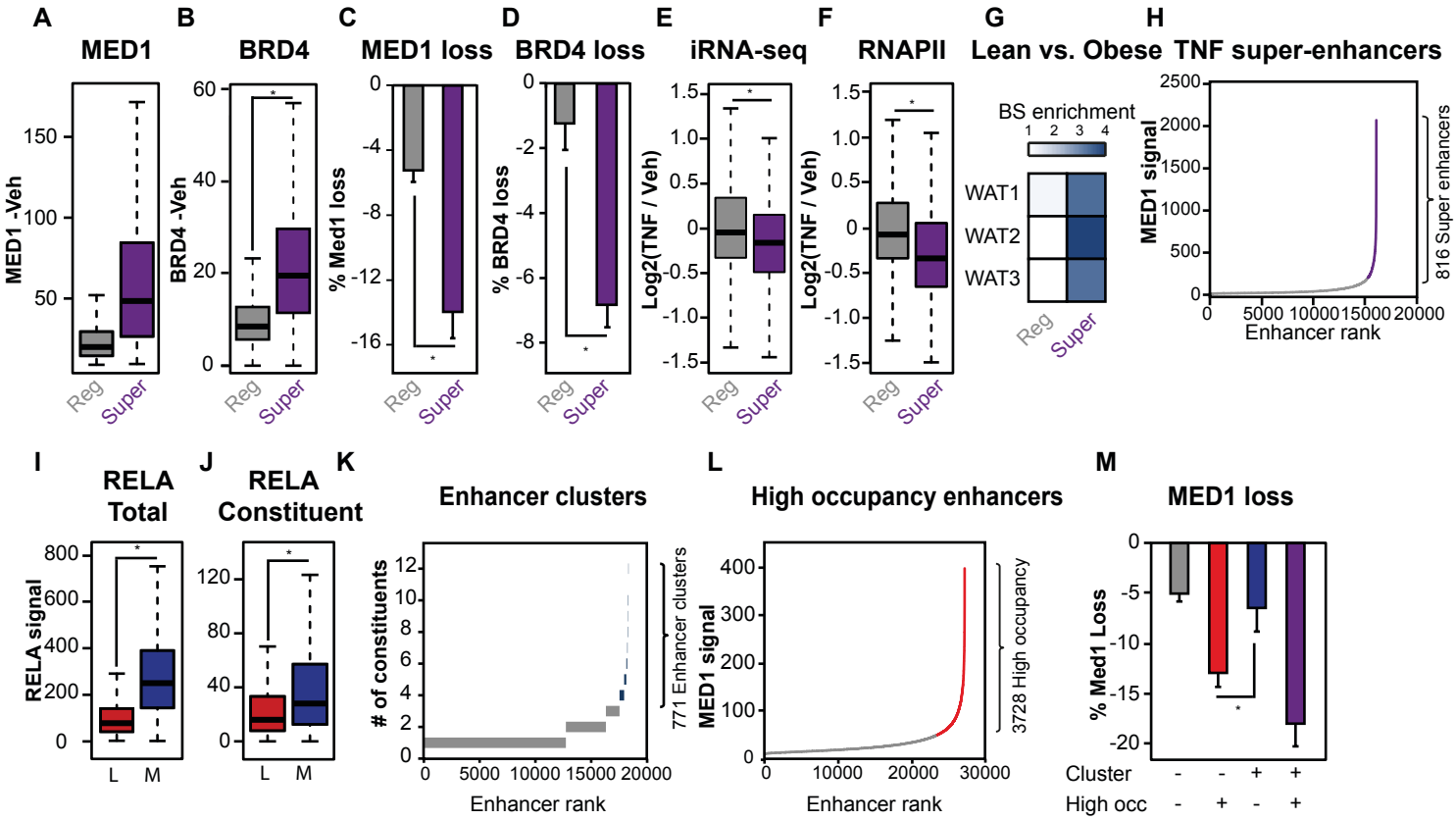


**Figure S4: Related to Figure 4**

Characterization of (super)-enhancers in SGBS adipocytes and their response to TNF exposure in terms of MED1 loss.

**A-B:** Boxplots showing MED1 (A) and BRD4 (B) occupancy in vehicle-treated cells at constituents of super-enhancers or regular enhancers as defined in Fig. 4A. p-value:*<2.2E-16, Wilcoxon rank sum test.

**C-D:** Bar diagrams representing mean % loss of MED1 (C) and BRD4 (D) binding following TNF exposure for regular enhancers (light grey) and super-enhancer (purple) constituents (defined in Fig. 4A). p-value:*<2.2E-16, Welch's t-test.

**E-F:** Boxplots representing log2 fold change in transcription as determined by intron RNA (E) or RNAPII ChIP-seq (F) read counts for genes within 20kb of regular (light grey) and super-enhancers (purple) constituents (defined in Fig. 4A).

**G:** Heatmaps representing the enrichment of regular- and super-enhancers defined in Fig. 4A within 20 kb of the TSS of the top 200 genes repressed in the adipose tissue of obese compared to lean subjects in three different studies: WAT1(Lee et al. 2005); WAT2 (Arner et al. 2012); and WAT3 (Tam et al. 2011). Enrichments are compared to the number of sites within 20 kb of constitutive genes.

**H:** Definition of super-enhancers in TNF-treated adipocytes (TNF super-enhancer). All identified MED1 (TNF) binding sites (23,167) within 12.5 kb of each other were merged resulting in 16,108 regions of which 816 were classified as super-enhancers in both MED1-TNF replicates based on input subtracted read counts.

**I-J:** Boxplots illustrating total (I) and per constituent (J) RELA occupancies at basal super-enhancers that are lost and maintained in response to TNF as defined in Fig. 4D. p-value:*<2.2E-16, Wilcoxon rank sum test.

**K:** Definition of enhancer clusters in vehicle treated All identified MED1 (vehicle) binding sites (27,123) within 12.5 kb of each other were merged, resulting in 18,224 regions of which (771 regions, blue) were defined as enhancer clusters (4+ constituents).

**L:** Definition of high occupancy enhancers. All identified MED1 (vehicle) binding sites (27,123) were ranked according to MED1 occupancy, and the top 3728 sites (red) corresponding to the total number of constituents in enhancer clusters defined in K.

**M:** Bar diagrams representing mean % loss of MED1 occupancy following TNF exposure for the enhancers defined as cluster and/or high occupancy enhancers in Fig. 4F.

# Fig. S5

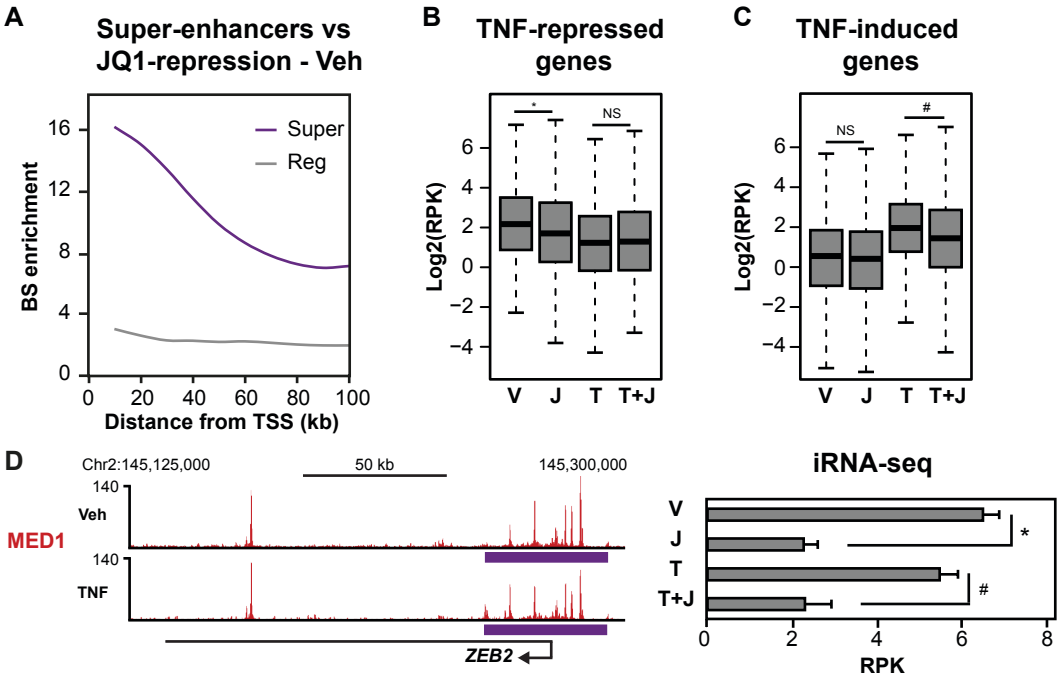


**Figure S5: Related to Figure 5**

**A:** Enrichment of basal regular- and super-enhancer constituents (defined in Fig. 4A) near genes repressed by JQ1 in vehicle-treated SGBS adipocytes (V vs J, FDR<0.01). Enrichment was determined as the number of binding sites per gene within different distances from the TSS (10–100 kb) of repressed genes (top 200 and all repressed) relative to the number of binding sites per constitutive gene (FDR>0.9 & abs(log2FC)<0.2).

**B-C:** Boxplots illustrating nascent transcript levels determined as intron read densities (reads per kb per 10 M read) at genes repressed (B) or induced (C) by TNF (as defined in Fig. 5B). p-values: *=8.48E-3, #= 2.69e-07, Wilcoxon rank sum test.

**D:** UCSC genome browser screenshots of MED1 occupancy at *ZEB2* locus which is associated with a maintained basal super-enhancer. The purple bar indicates the position of the super-enhancer. FDR: *= 6.39E-07, #= 1.08E-08, EdgeR.

# Fig. S6

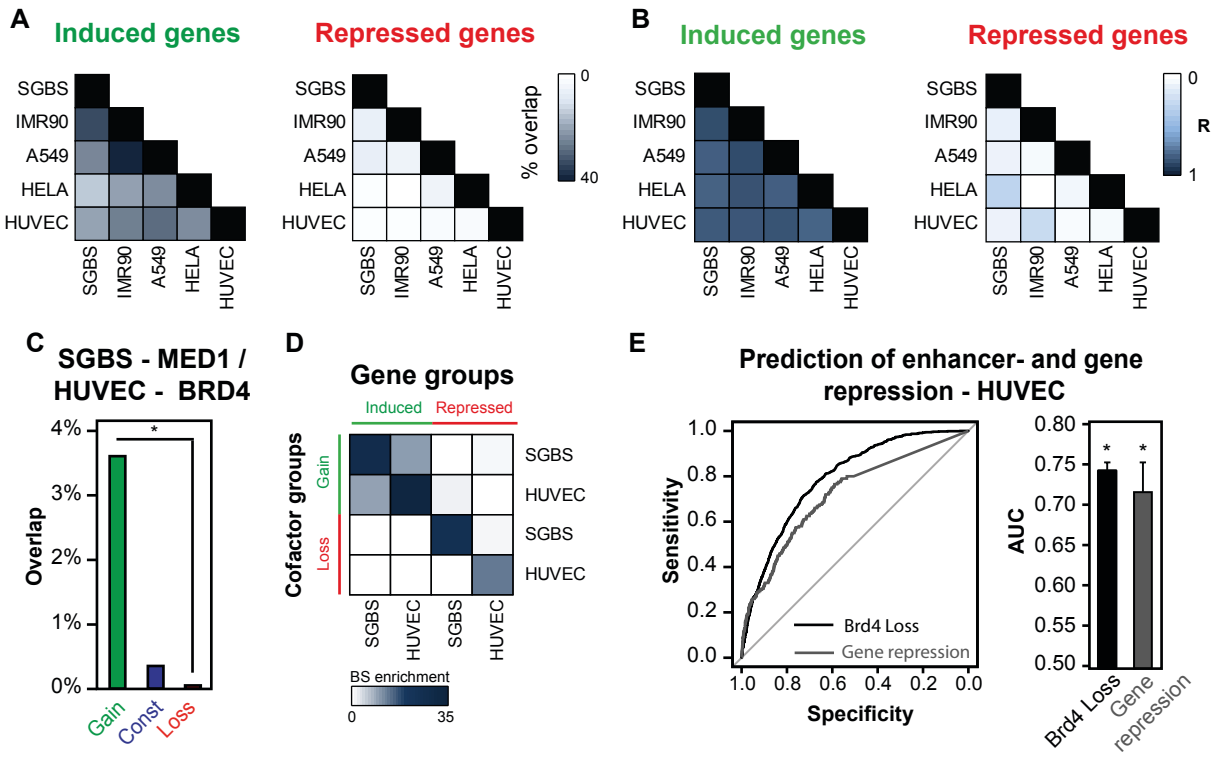


**Figure S6: Related to Figure 6**

Comparison of TNF-regulated gene programs in different human cell types.

**A:** Heatmap representing % overlap between top 200 TNF-induced (left) or repressed (right) genes in 5 different human cell types.

**B**. Heatmaps showing correlation between TNF-regulated pathways in 5 human cell types. -Log(p-values) for the enrichment of the top 500 TNF-induced (left) or -repressed (right) genes in each pathways were determined for each of the 219 wikipathways categories, and the pairwise Pearson correlation coefficients of the -log(p-values) for all cell type pairs were determined.

**C:** Bar diagram representing the overlap between TNF-regulated MED1 sites in SGBS cells and TNF-regulated BRD4 sites in SGBS/HUVEC cells. The top 2000 regulated enhancers in each cell type were compared. p-value *<2.2E-16, Pearson Chi-squared test.

**D:** Heatmap representing enrichment of cofactor binding sites (with gain or loss of cofactor) as defined in SGBS and HUVEC cells within 20kb of the TSS of TNF regulated genes in SGBS and HUVEC cells. Enrichment is relative to the number of sites within 20kb of the TSS of constitutive genes (FDR/P>0.9)

**E:** ROC-curves for prediction of the top 2000 enhancers with loss of BRD4 (dark grey) and top 200 genes (light grey) repressed by TNF in HUVECs based on BRD4 occupancy in vehicle-treated cells and RELA occupancy in TNF-treated cells similar to the models defined by MED1 and RELA occupancies in SGBS adipocytes (Fig. 4F,G). Bar diagrams represent the AUC for each ROC-curve with error bars representing the 95% confidence interval of the AUC determined by DeLongs test. p-value*<2.2E-16, DeLongs test.

# Table S1

**A**

| Pathway | logP (iRNA) | logP (RNAPII) | Genes |
|---|---|---|---|
| TWEAK Signaling | -17.6 | -20.7 | TNF, BIRC3, CCL2, CCL5, BIRC2, TRAF1, IL6, NFKB1, NFKBIA, RELB, TRAF3, NFKB2, NFKBIB, TRAF1 |
| TNF Signaling | -15.7 | -17.5 | TNF, TNFAIP3, BIRC3, NFKBIE, MAP3K8, BID, BIRC2, MAP2K3, TNFRSF1B, TRAF1, IL6, MAP2K6, NFKBIA, NFKB1, MAP3K5, NFKB2, NFKBIB, MAP3K1 |
| Senescence and Autophagy | -13.2 | -11.2 | FN1, IL1B, MAP1LC3A, AMBRA1, MAP2K3, THBS1, IGFBP7, SQSTM1, IL6, IL6ST, IL8, CXCL1, BCL2, HMGA1, CD44, IRF1 |
| Regulation of TLR signaling | -11.3 | -14.4 | TNF, IFNAR2, CYLD, TNFAIP3, MAP3K8, IRAK3, IFNAR1, CCL5, IL1B, MAP2K3, IKBKE, SQSTM1, IL6, MAP2K6, NFKBIA, NFKB1, IL8, TRAF3, LBP, NFKB2 |
| Apoptosis | -11.1 | -20.2 | TNF, NFKBIE, BIRC3, BID, BIRC2, FAS, TNFRSF1B, NFKB1, NFKBIA, TRAF3, BCL2, NFKBIB, MAP3K1, IRF1, TRAF1 |
| RANKL-RANK Signaling | -10.2 | -14.6 | TRAF1, PAPSS2, SQSTM1, MAP2K6, NFKBIA, NFKB1, RELB, TRAF3, VCAM1, TNFRSF11B, NFKB2, ICAM1 |

**B**

| Pathway | logP (iRNA) | logP (RNAPII) | Genes |
|---|---|---|---|
| Triacylglyceride Synthesis | -7.2 | -2.5 | GPAM, AGPAT2, DGAT1, MOGAT1, PNPLA2, DGAT2 |
| FA, TAG, and KB metabolism | -7.1 | -5.6 | ACSL5, ACACB, TBL1XR1, ELOVL6, RXRA, DGAT2, FASN |
| Adipogenesis | -6.7 | -5.6 | RXRG, SLC2A4, AGPAT2, PPARG, CISD1, RXRA, WWTR1, SREBF1, PCK1, GATA3, MEF2D, PNPLA3, ADIPOQ, RBL2, PLIN1 |
| AMPK signaling | -6.3 | -1.1 | PFKFB3, ACACB, SLC2A4, ADIPOQ, EIF4EBP1, PIK3R1, SREBF1, ADIPOR2, FASN |
| Fatty Acid Biosynthesis | -5.7 | -7.2 | ACSL5, ACACB, ACSS2, ECHDC1, FASN |
| Glycogen Metabolism | -5.0 | -5.3 | PYGL, PPP2R5A, PHKA2, GYG2, PHKG1, PYGB |

**Table S1: Related to Figure 1**

**A-B :** Tables representing log(p-values) for the top 6 enriched pathways for genes induced (A) and repressed (B) by TNF as assessed by iRNA-seq (defined in Fig. 1A). The tables also include log(p-values) for the enrichments of these pathways amongst genes induced (n=816) or repressed (n=265) by TNF as assessed by RNAPII ChIP-seq (FDR<0.01). Genes identified as differentially expressed by both iRNA-seq and RNAPII ChIP-seq are listed for each pathway.

# Table S2

**A**

| RNA primers | Forward | Reverse |
|---|---|---|
| PPARG mRNA | AGCAAACCCCTATTCCATGCT | ATCAGTGAAGGAATCGCTTTCTG |
| TNF mRNA | ATCTTCTCGAACCCCGAGTGA | GGGTTTGCTACAACATGGGCTA |
| IL1A mRNA | AAGAGACGGTTGAGTTTAAGCCA | GGCCTCCAGGTCATCATCAGT |
| SREBF1 mRNA | ACTTCTGGAGGCATCGCAAGCA | AGGTTCCAGAGGAGGCTACAAG |
| CEBPA mRNA | AACCTTGTGCCTTGGAAATG | CTGTAGCCTCGGGAAGGAG |
| TLE3 mRNA | CCACCATGAACTCGATCACAGAG | CTTGGCTTCCATGCTGTAGTCC |
| RXRG mRNA | GTGAGCTGGACTCTGGATCG | CCCTGGTAAGGGCTTGATGT |
| RELA mRNA | TTGCTGTGCCTTCCCGCAGC | ATAGGGCTGGCGTGCTGGCTT |
| TBP mRNA | GCCCGAAACGCCGAATAT | CCTCATGATTACCGCAGCAAA |
| PPARG pre-mRNA | ATCCAGTGGTTGCAGATTAC | AGAGATGAGTCCAATTCTAGTCC |
| NFKBIA pre-mRNA | GCAAATAGCAGAGGCTCCAG | TCACATCAGCCCACATCCTA |
| IRF1 pre-mRNA | TGAAGGAGGAAGGCAAGGTA | TTGACCACTGTGGCTCTCTG |
| TNFAIP2 pre-mRNA | GCGTGAGTGAGCCACTTG | GGTGAAAGCAGGGAGACAGA |
| NFKB2 pre-mRNA | CAGCGAGGGAGACTATGAGG | AGAGCATCCTTCGCTTTCAA |
| TNFAIP3 pre-mRNA | TCTGTGACAGTCCCAAACCA | AGGATTTTCTGCCCTTGGAC |
| ZC3H12A pre-mRNA | AGGCAGGCTGATGAGTCAGT | GTCCATGCCAACAGGAACTT |
| ADM pre-mRNA | AGCAGTTTCCAGCTCCCTCT | ACTTGAGACCCCATCAAGCA |
| PPP1R15B pre-mRNA | CCATGTGGAGCCAAGAGATT | TGACCTCAGATTCTGCCTCAC |
| REPIN1 pre-mRNA | TAGACTGCCGGGAGTAGCAC | GAGGCTGGAGGACAAGTGAG |
| VIM pre-mRNA | AGGGTGAAAAGGAGCCATCT | AGTGAAGCCCATAGAAACCA |
| HK2 pre-mRNA | CCAGCCTGGCCTGCCTTTGTTT | AGATCTTTCACACGCACATTTGGCA |
| ACACB pre-mRNA | ACATGCTCTGAAATGAGCACGGT | TGGGATCACACAGAACAGGAGGT |
| CIDEC pre-mRNA | GTTACACGGGCCACATCAAT | TCAAGGGGTGCTAACCATTT |
| FABP4 pre-mRNA | TGATGATCATGTTAGGTTTGG | AATCTGACATCTTTTCTTTTCC |
| PCK1 pre-mRNA | CGGCTGAAGAAGTATGACAA | CTTCATTCACCTTTCTCCAC |
| PLIN1 pre-mRNA | ATCTCCCCTCCCTGCTTCTT | CAACAAAGGCCTCACCTTGC |
| STOM pre-mRNA | ACACAGGCTGATTAGTCCAGAGGGC | AGCTGATGGGGAACGGGGACAA |
| MARC1 pre-mRNA | TGTTACTGGGGGCTGGGGGAAG | TCACCCCAAACAGAAACTCTGTACCA |
| OSBPL11 pre-mRNA | GACTCCCGGCTCTCTCCAGACC | CGTCCTGACCTGCTATGGGGCT |
| DGAT2 pre-mRNA | CCAATTCCGTGTGGCTTCCCCC | TTGGTGACGCAGCCCCAAAGTG |
| CFH pre-mRNA | CTCACTAGGAAGTGAGCGGG | CATAACAACACAATCCCCGGC |
| CTSZ pre-mRNA | CCTGCTGAATGAAGGGCTGA | TCGTTCACAGAGCTGACACC |
| LYRM4 pre-mRNA | TGGAACGCCTCCTTATGCAA | TAAGCACACCAGCACCCTAC |
| TMEM170B pre-mRNA | AAAGTTGATATTTGGACCTCTTCTC | TGTGTAAGAAGGCTAAAACTGCC |
| VSTM4 pre-mRNA | GTGCCCCCATGACCTTTACA | AAAGGAAGAGCTTCCCTCGC |

**B**

| ChIP primers | Forward | Reverse |
|---|---|---|
| Loss#1 | CTTACTGCACCCTCCTCAGC | TCTCGGAACAAATGCAATCA |
| Loss#2 | CTTACTGCACCCTCCTCAGC | TCTCGGAACAAATGCAATCA |
| Loss#3 | GAGCTTGGCAGAGCTAGAAGA | TGGTGTGTTTGCTTTTCAGG |
| Loss#4 | GGACTTCGCTCCTTCCTTCT | AGAGCTGTGTTGCACTGACC |
| Loss#5 | CCAGATGCCATTCCTCAAAT | TGGGTAGAGGGCACTACAGG |
| Loss#6 | GGACTTCGCTCCTTCCTTCT | AGAGCTGTGTTGCACTGACC |
| Loss#7 | TAGGGGCAAAATACCCTTGG | CCATGTATGTGTGTGCGTGA |
| Loss#8 | CATCTCATTTGCTGCCAAAC | CCGGCTATTCTCTGGTTTCA |
| Gain#1 | CGTGGGGTACACTTTGTCTG | AAATGTTTCAGGGCCTGTTG |
| Gain#2 | TTCATCAGCGGATACAAGTGA | TGGGGGTAAGACCTTACGAA |
| Gain#3 | GCTGTGCATTCCTTCCTTTC | CCCCAGAGTCTTCACAGCAT |
| Gain#4 | AAAAGTCAGGGTTGGGGAAG | TCCCTCTTGAGCTTCTCTGG |
| Gain#5 | TGCAGAGGGGAAATTCTTTG | AATGCCCTCAACATCTCACC |
| Gain#6 | GTCAGCCATGGTCCGTTGGGTTC | TCAGGTAACGAGGGTGTCAGGGC |
| Gain#7 | TGTGGGGATGGGGGATCCAGAAC | AAAGGCTTTGTCCTGCCCCTCCT |

**C**

| pSico shRNA oligoes | |
|---|---|
| shScr S | TGAAATCTATTGTCCATATA*TTCAAGAGA*TATATGGACAATAGATTCC**TTTTTTC** |
| shScr AS | TCGA **GAAAAAA**GGAATCTATTGTCCATATA*TCTCTTGAA*TATATGGACAATAGATTTCA |
| shRELA S | TCGGATTGAGGAGAAACGTAAA*TTCAAGAGA*TTTACGTTTCTCCTCAATCCG**TTTTTTC** |
| shRELA AS | TCGAGAAAAAACGGATTGAGGAGAAACGTAAA*TCTCTTGAA*TTTACGTTTCTCCTCAATCCGA |

**Table S2: Related to Figure S1, Figure 2, and Figure S2**

**A-B:** Sequences of qPCR primers used for RNA (A) (Fig. S1A,B,E,G, Fig. S2A) and ChIP (B) (Fig. 2C) experiments. **C:** Sequences of shRNA oligos cloned into pSico used for RELA depletion (Fig. 2A,B; Fig. S2A)

# Table S3

**A**

| Study | Accession | Platform Expression | Source |
|---|---|---|---|
| **(Lee et al. 2005)** | GSE2508 | HG_U95A-E & HG_U95Av2 Arrays | Abdominal subcutaneous adipocytes |
| **(Arner et al. 2012)** | GSE25402 | HuGene-1_0-st Array | Abdominal subcutaneous adipose tissue |
| **(Tam et al. 2011)** | GSE29718 | HuGene-1_0-st | Subcutaneous adipose tissue |

**B**

| Study | (Madsen et al. 2015) | (Jin et al. 2013) | (Yang et al. 2013) | (Rao et al. 2011) | (Brown et al. 2014) |
|---|---|---|---|---|---|
| **Accession** | GSE60462 | GSE43070 | SRP020499 | GSE24518 | GSE53998 |
| **Cell line** | SBGS | IMR90 | A549 | HeLa | HUVEC |
| **Gene expression** | Total RNA-seq + iRNA-seq | Total RNA-seq + iRNA-seq | Total RNA-seq + iRNA-seq | RNAPII ChIP-seq | RNAPII ChIP-seq |
| **Cofactor** | MED1 | - | - | - | BRD4 |
| **TNF conc.** | 10ng/mL | 10ng/mL | 30ng/mL | 10ng/mL | 25ng/mL |
| **TNF duration** | 90 min | 60 min | 60 min | 60 min | 60 min |
| **TNF Source** | Human Rec. (Invitrogen) | Human Rec. (R&D Systems) | Human Rec. (Pepro Tech) | Human Rec. (Sigma-Aldrich) | Human Rec. (Pepro Tech) |
| **Serum starvation** | Yes – Serum free diff. | No | No | Charcoal-stripped FCS 72hrs | No |

**Table S3: Related to Figure S4 and Figure 6**

**A-B:** Overview of publically available datasets from the study of gene expression in human lean vs obese adipose tissue (A)(Supplemental Fig. S4G) and acute gene regulation by TNF in different human cell types (B) (Fig. 6)

# Supplemental Methods

***RNA-seq analysis***

All RNA-seq reads were mapped to the hg19 genome with STAR (Dobin et al. 2013) using default parameters. Read quantification and differential expression analysis were performed using the iRNA-seq pipeline (Madsen et al. 2015) with significance cutoffs as specified in the individual figures. Top200 or -500 genes were selected based on lowest FDR-values. Functional enrichment analysis was performed with HOMER (Heinz et al. 2010).

***ChIP- and DNase-seq analysis***

ChIP-seq and DNAse-seq data were mapped to the hg19 genome with STAR (Dobin et al. 2013), and further analyzed using HOMER (Heinz et al. 2010). Tag directories were generated by calling makeTagDirectory specifying -tbp 1 and -normGC default, and peak detection was performed on pooled libraries of replicate experiments using findPeaks -style factor. MED1 peak files from vehicle and TNF-treated adipocytes were subsequently merged, and reads within 400 bp around the center of each peak were quantified for each replicate of each condition. EdgeR (Robinson et al. 2010) was used for normalization across replicates and conditions, and the merged peak file was filtered to obtain peaks with minimum 8 normalized tags in both replicates of minimum one condition. Following filtering, EdgeR was used for calling differential MED1 occupancy (FDR<0.01). HOMER was used to quantify reads of other factors/DNase-seq within a 400bp window for boxplots and for aggregate plots as specified in the individual figures. A pseudo count of 1 was added before calculation of changes in occupancy to avoid small numbers effects, and sites with less than 6 tags per 10 M in both conditions were removed from the analysis. Intersections between genomic position files were generated using BEDTools (Quinlan 2014), and the UCSC genome browser (Kent et al. 2002) was used for data visualization.

***eRNA analyses***

RNA-seq signal in 50bp bins was quantified in a 3kb window around the center of all intergenic random or MED1 binding sites and normalized to 10 M reads using HOMER. Sites with an RNA-seq signal in a single bin exceeding 2 normalized tags were removed before the average signal for each bin was calculated and plotted as aggregate plots for each MED1 group. For boxplots, HOMER was used to count RNA-seq signal in a 2kb window around all intergenic MED1 sites, and sites with less than 1 normalized tag per 10 M in both vehicle and TNF sample were removed. The normalized tag counts were adjusted by empirical Bayes shrinkage estimation using EdgeR and fold changes between vehicle and TNF were calculated and plotted. Random sites were obtained by shuffleBED function in BEDTools using all intergenic MED1 sites as input. Genomic gaps and all GENCODE-annotated genes were excluded from this file.

***Calculation of binding site enrichment***

We identified the TSS of the genes in each group and generated genomic coordinates. The TSS was extended in bins of 10kb from 0kb up to 100kb in each direction using slopBED. The number of binding sites per extended TSS bin was determined using the intersectBED function in BEDTools, and an average number calculated for each gene group. The enrichment scores for regulated genes were calculated relative to constitutive genes.

***Prediction of changes in enhancer activity and gene regulation***

All ROC-curves were generated using the pROC package for R (Robin et al. 2011). 95% confident intervals for AUC for each ROC-curve were calculated using de Longs test (DeLong et al. 1988). Before subtraction of MED1 and RELA occupancies, these were centered and scaled using the scale function in R. For prediction of gene regulation, (subtracted) factor occupancies were multiplied by a distance score for each promoter-enhancer pair calculated using the formula: Distance score = exp(-0.5+4*d/100000), where d is the distance (in bp) from promoter to enhancer (Tang et al. 2011). Only enhancers within 100kb of a TSS were considered.

***Identification of super-enhancers***

For identification of super-enhancers, MED1 peaks, identified as described above, were stitched together if they were positioned within 12,500 bp. These stitched regions were used for quantification of MED1 and input reads, and regions were ranked and classified according to input-subtracted MED1 occupancies as previously described (Whyte et al. 2013). Regions identified as super-enhancers in both replicates were used for further analysis and all other denoted as regular enhancers.

***Microarray analyses***

We identified 3 individual studies of lean and obese human adipose tissue. Data was extracted from Gene Expression Omnibus (GEO) using GEO2R online tool (Barrett et al. 2013) to compare lean and obese datasets. Microarray probe IDs were matched to Ensemble annotated genes using Archive Ensemble (Feb2014, GRCh37/hg19) Biomart online tool. Coordinates of the top 500 repressed genes (ranked by p-value), and constitutively expressed genes in the individual studies were extracted for further analysis.

# Supplemental References


Arner E, Mejhert N, Kulyte A, Balwierz PJ, Pachkov M, Cormont M, Lorente-Cebrian S, Ehrlund A, Laurencikiene J, Heden P et al. 2012. Adipose tissue microRNAs as regulators of CCL2 production in human obesity. *Diabetes* **61**(8): 1986-1993.

Barrett T, Wilhite SE, Ledoux P, Evangelista C, Kim IF, Tomashevsky M, Marshall KA, Phillippy KH, Sherman PM, Holko M et al. 2013. NCBI GEO: archive for functional genomics data sets--update. *Nucleic acids research* **41**(Database issue): D991-995.

Brown JD, Lin CY, Duan Q, Griffin G, Federation AJ, Paranal RM, Bair S, Newton G, Lichtman AH, Kung AL et al. 2014. NF-kappaB Directs Dynamic Super Enhancer Formation in Inflammation and Atherogenesis. *Molecular cell* **56**(2): 219-231.

DeLong ER, DeLong DM, Clarke-Pearson DL. 1988. Comparing the areas under two or more correlated receiver operating characteristic curves: a nonparametric approach. *Biometrics* **44**(3): 837-845.

Dobin A, Davis CA, Schlesinger F, Drenkow J, Zaleski C, Jha S, Batut P, Chaisson M, Gingeras TR. 2013. STAR: ultrafast universal RNA-seq aligner. *Bioinformatics* **29**(1): 15-21.

Heinz S, Benner C, Spann N, Bertolino E, Lin YC, Laslo P, Cheng JX, Murre C, Singh H, Glass CK. 2010. Simple combinations of lineage-determining transcription factors prime cis-regulatory elements required for macrophage and B cell identities. *Molecular cell* **38**(4): 576-589.

Jin F, Li Y, Dixon JR, Selvaraj S, Ye Z, Lee AY, Yen CA, Schmitt AD, Espinoza CA, Ren B. 2013. A high-resolution map of the three-dimensional chromatin interactome in human cells. *Nature* **503**(7475): 290-294.

Kent WJ, Sugnet CW, Furey TS, Roskin KM, Pringle TH, Zahler AM, Haussler D. 2002. The human genome browser at UCSC. *Genome research* **12**(6): 996-1006.

Lee YH, Nair S, Rousseau E, Allison DB, Page GP, Tataranni PA, Bogardus C, Permana PA. 2005. Microarray profiling of isolated abdominal subcutaneous adipocytes from obese vs non-obese Pima Indians: increased expression of inflammation-related genes. *Diabetologia* **48**(9): 1776-1783.

Madsen JG, Schmidt SF, Larsen BD, Loft A, Nielsen R, Mandrup S. 2015. iRNA-seq: computational method for genome-wide assessment of acute transcriptional regulation from total RNA-seq data. *Nucleic acids research* **43**(6): e40.

Quinlan AR. 2014. BEDTools: The Swiss-Army Tool for Genome Feature Analysis. *Current protocols in bioinformatics / editoral board, Andreas D Baxevanis [et al]* **47**: 11 12 11-11 12 34.

Rao NA, McCalman MT, Moulos P, Francoijs KJ, Chatziioannou A, Kolisis FN, Alexis MN, Mitsiou DJ, Stunnenberg HG. 2011. Coactivation of GR and NFKB alters the repertoire of their binding sites and target genes. *Genome research* **21**(9): 1404-1416.

Robin X, Turck N, Hainard A, Tiberti N, Lisacek F, Sanchez JC, Muller M. 2011. pROC: an open-source package for R and S+ to analyze and compare ROC curves. *BMC bioinformatics* **12**: 77.

Robinson MD, McCarthy DJ, Smyth GK. 2010. edgeR: a Bioconductor package for differential expression analysis of digital gene expression data. *Bioinformatics* **26**(1): 139-140.

Tam CS, Heilbronn LK, Henegar C, Wong M, Cowell CT, Cowley MJ, Kaplan W, Clement K, Baur LA. 2011. An early inflammatory gene profile in visceral adipose tissue in children. *International journal of pediatric obesity : IJPO : an official journal of the International Association for the Study of Obesity* **6**(2-2): e360-363.

Tang Q, Chen Y, Meyer C, Geistlinger T, Lupien M, Wang Q, Liu T, Zhang Y, Brown M, Liu XS. 2011. A comprehensive view of nuclear receptor cancer cistromes. *Cancer research* **71**(22): 6940-6947.

Whyte WA, Orlando DA, Hnisz D, Abraham BJ, Lin CY, Kagey MH, Rahl PB, Lee TI, Young RA. 2013. Master transcription factors and mediator establish super-enhancers at key cell identity genes. *Cell* **153**(2): 307-319.

Yang J, Mitra A, Dojer N, Fu S, Rowicka M, Brasier AR. 2013. A probabilistic approach to learn chromatin architecture and accurate inference of the NF-kappaB/RelA regulatory network using ChIP-Seq. *Nucleic acids research* **41**(15): 7240-7259.